

# A Lower Estimate of the Topological Entropy from Reconstructed Time Series

Maria Vivien V. Visaya\*

## Abstract

We present a simple method applied to a time series that will reveal something about the underlying dynamics that drives it. In particular, we give a lower bound to the topological entropy of the unknown dynamical system via a one-dimensional multivalued map obtained from the time series. The method is illustrated using the Hénon map and the magnetoelastic ribbon data.

**Keywords:** Time series; Topological entropy; Multivalued maps; Reconstruction; Continuous selectors

## 1 Introduction

Let  $f : \mathcal{M} \rightarrow \mathcal{M}$  be an unknown dynamical system acting on a compact domain of  $\mathbb{R}^d$  or a finite-dimensional compact manifold  $\mathcal{M}$ . Given a sequence of successive iterates  $\{x_n\}_{n \in \mathbb{N}}$  of a point  $x_0 \in \mathcal{M}$ , where  $x_n = f^n(x_0)$ , define an observation function  $\rho : \mathcal{M} \rightarrow \mathbb{R}$  which is continuous and which assigns to each state  $x_n \in \mathcal{M}$  the corresponding observation  $\rho(x_n) \in \mathbb{R}$ . We shall call this sequence  $\{u_n\}$  a *time series*. The relationship between  $\{u_n\}$  and  $f$  is  $u_n = \rho(x_n) = \rho(f^n(x_0))$ .

In the case where  $\{u_n\}$  is given by an observation of some experiment,  $\{x_n\}$  is often difficult to observe. Hence, understanding  $\{u_n\}$  is crucial if we want to infer some interesting idea about how the *true* underlying system behaves.

---

\*Department of Mathematics, Faculty of Science, Kyoto University, Kyoto 606- 8502.  
v3isaya@math.kyoto-u.ac.jp

The notion of topological entropy, an invariant quantitative measure of the complexity of a dynamical system  $f$ , is often used to define chaos. It measures the extent to which points that are very near are mapped to points that are far away by repeated application of  $f$ . A dynamical system  $f$  may be said to be chaotic if its topological entropy, denoted by  $h_{\text{top}}(f)$ , is positive.

In this paper, we present a means of estimating a lower bound of the topological entropy of  $f$  via a time series  $\{u_n\}$ . In doing so, we employ the method of time-delay reconstruction and consider a set-valued map, which we shall refer to as a *multivalued map*, obtained from the time series. We then give a condition on the multivalued map that implies the positivity of  $h_{\text{top}}(f)$ . We also show that in some cases, a one-dimensional reconstruction is enough to say something about the complexity of the unknown dynamical system  $f$ .

This paper is organized as follows. In Section 2, we introduce terminologies that are important to understand our results. We present two theorems in Section 3. In Section 4, an application to the Hénon map and magnetoelectric ribbon data is presented. We give concluding remarks in Section 5. Further study on the definition of topological entropy for multivalued maps is given in section 6.

## 2 Basic Terminologies

**Definition 2.1** Let  $(X, d)$  be a compact metric space with distance  $d$  and let  $g : X \rightarrow X$  be continuous. For any integer  $k \geq 1$ , define the distance function  $d_k : X \times X \rightarrow \mathbb{R}_{\geq 0}$  by

$$d_k(x, y) = \max_{0 \leq \ell < k} d(g^\ell(x), g^\ell(y)).$$

A finite set  $E \subset X$  is called  $(k, \delta)$ -separated if  $d_k(x, y) \geq \delta$  for all  $x, y \in E$ . Moreover, if  $E$  has the maximal cardinality among all the  $(k, \delta)$ -separated sets, then  $E$  is called a *maximal  $(k, \delta)$ -separated set*. The topological entropy of  $g$  is given by

$$h_{\text{top}}(g) = \lim_{\delta \rightarrow 0} \limsup_{k \rightarrow \infty} \frac{\log s_g(k, \delta)}{k},$$

where  $s_g(k, \delta)$  is the cardinality of the maximal  $(k, \delta)$ -separated set for  $g$ .

This standard definition of the topological entropy for continuous maps on a compact metric space is due to Bowen [4].

**Definition 2.2** Let  $X$  and  $Y$  be arbitrary sets. A *multivalued map*  $F$  from  $X$  to  $Y$ , denoted by  $F : X \rightrightarrows Y$ , is such that  $F(x)$  is assigned a set  $Y_x \subset Y$  for all  $x \in X$ . A single-valued map  $g : X'(\subset X) \rightarrow Y$  is called a *selector* for  $F$  over  $X'$  if  $g(x) \in F(x)$  for all  $x \in X'$ .

**Definition 2.3** Let  $X$  and  $Y$  be topological spaces and let  $F : Y \rightrightarrows Y$  be a multivalued map. Let  $f : X \rightarrow X$  and  $q : X \rightarrow Y$  be continuous single-valued maps. The following diagram is said to *upper-semicommute* if  $q(f(x)) \in F(q(x))$  holds for any  $x \in X$ :

$$\begin{array}{ccc} X & \xrightarrow{f} & X \\ q \downarrow & F & \downarrow q \\ Y & \rightrightarrows & Y \end{array}$$

In the setting given above, namely given  $f : \mathcal{M} \rightarrow \mathcal{M}$  and  $\rho : \mathcal{M} \rightarrow \mathbb{R}$ , let  $I = \rho(\mathcal{M})$  be the image of  $\rho$ . We then define a multivalued map  $\mathcal{F} : I \rightrightarrows I$  by

$$\mathcal{F}(x) = (\rho \circ f)(\rho^{-1}(x)) \quad (1)$$

such that the diagram

$$\begin{array}{ccc} \mathcal{M} & \xrightarrow{f} & \mathcal{M} \\ \rho \downarrow & \mathcal{F} & \downarrow \rho \\ I & \rightrightarrows & I \end{array} \quad (2)$$

upper-semicommutates. Thus, for a time series  $\{u_n\}$  given by  $u_n = \rho(x_n) = \rho(f^n(x_0))$ , it follows that the relation between  $\mathcal{F}$  and  $\{u_n\}$  is such that  $u_{n+1} \in \mathcal{F}(u_n)$ .

**Definition 2.4** Let  $\mathcal{F} : \mathbb{R} \rightrightarrows \mathbb{R}$  be a multivalued map and let  $J, K$  be compact intervals. Let  $\partial^-(J)$  and  $\partial^+(J)$  denote the left and right boundaries of  $J$ , respectively, and let  $K^- = \{x \mid x < \min(K)\}$  and  $K^+ = \{x \mid x > \max(K)\}$ . The interval  $J$  is said to  *$\mathcal{F}$ -cover*  $K$  if the following conditions are satisfied:

- 
- Figure 1 consists of two 4x4 grids, (a) and (b), illustrating the definition of  $J_1$  and  $J_2$ . In both grids, the bottom two rows are shaded gray and labeled  $J_1$  on the left. The top two rows are labeled  $J_2$  on the left. A vertical bracket on the far left of grid (a) spans the top two rows and is labeled  $K$ . In grid (a), a black curve starts at the bottom left, goes up to the top right, and then back down to the bottom right. In grid (b), the curve starts at the bottom left, goes up to the top right, and then back down to the bottom right, but with a different shape, showing a more pronounced peak in the top right corner.

### 3 Statement of Results

(\*) there exist disjoint compact subintervals  $J_1, J_2, \dots, J_\ell$  of  $I$  and  $K \supset J_1 \cup J_2 \cup \dots \cup J_\ell$  such that for any  $i = 1, 2, \dots, \ell$ ,  $J_i$   $\mathcal{F}$ -covers  $K$ .

4

The basic idea of Theorem 1 is that given a time series  $\{u_n\}$  observed from  $f$  and a multivalued map  $\mathcal{F}$  obtained from  $\{u_n\}$ , we can say something about the complexity of the true underlying system  $f$  as long as certain geometric assumptions are satisfied, namely there is horseshoe-like dynamics present in  $\mathcal{F}$ .

We shall extend Theorem 1 for the subshift of finite type.

**Definition 3.1** Let  $\mathcal{F} : I \rightrightarrows I$  be a multivalued map on an interval  $I$  and let  $\{J_1, J_2, \dots, J_\ell\}$  be a set of compact disjoint subintervals of  $I$ . An  $\ell \times \ell$  matrix  $A = (a_{ij})$ ,  $a_{ij} \in \{0, 1\}$ , is a *transition matrix* for  $\mathcal{F}$  if for any  $i = 1, 2, \dots, \ell$ , there is an interval  $K_i \subset I$  such that for all  $a_{ij} = 1$ , the following conditions are satisfied:

1.  $K_i \supset J_j$
2.  $J_i$   $\mathcal{F}$ -covers  $K_i$ .

**Theorem 2.** Let  $f$ ,  $\mathcal{M}$  and  $\rho$  be as in Theorem 1. Let  $\mathcal{F} : I \rightrightarrows I$  be a multivalued map over an interval  $I$  and let  $\{J_1, J_2, \dots, J_\ell\}$  be a set of compact disjoint subintervals of  $I$ . Denote by  $\text{sp}(A)$  the spectral radius of  $A$ . If  $A$  is a transition matrix for  $\mathcal{F}$ , then  $h_{\text{top}}(f) \geq \log \text{sp}(A)$ .

### 3.1 Sketch of Proofs

For the sketch of the proof of Theorem 1, we consider the case  $\ell = 2$ . The proof can be readily extended to the general case and is treated in exactly the same manner. Let  $\rho^{-1}(J_i) = \mathcal{N}_i$  for any  $i = 1, 2$ . Then by the continuity of  $\rho$ , the compactness of the disjoint intervals, and the compactness of  $\mathcal{M}$ , each  $\mathcal{N}_i$  is compact and  $\mathcal{N}_1 \cap \mathcal{N}_2 = \emptyset$ . Figure 2 shows possible pre-images of  $J_1$  and  $J_2$  in  $\mathcal{M}$ .

The following Lemma is needed to prove Theorem 1.

**Lemma.** *There exists a continuous curve  $\alpha_i : [-1, 1] \rightarrow \mathcal{N}_i$  such that  $\rho(\text{Im}(\alpha_i)) = J_i$  and  $\rho(\alpha_i(\pm 1)) = \partial^\pm(J_i)$  for  $i = 1, 2$ .*

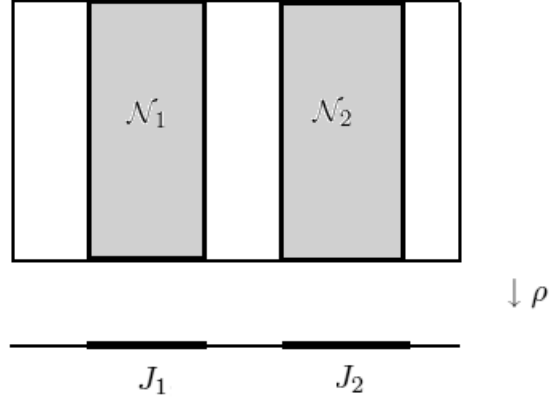


Figure 2: Pre-image in  $\mathcal{M}$  for the intervals  $J_1$  and  $J_2$ .

**Proof of Theorem 1.** Let  $\mathcal{N} = \mathcal{N}_1 \cup \mathcal{N}_2$  and let  $S^+ = \bigcap_{i=0}^{\infty} f^{-i}\mathcal{N}$ . This invariant set  $S^+$  is our object of interest so we study the restriction  $f|S^+$  and understand how the orbit of  $x \in S^+$  visits  $\mathcal{N}$  in time.

Let  $\Sigma_2^+ = \{s = (s_0, s_1, s_2, \dots, s_n, \dots) \mid s_i \in \{1, 2\} \text{ for all } i \in \mathbb{N}\}$  and  $\sigma : \Sigma_2^+ \rightarrow \Sigma_2^+$  be the shift map such that  $(\sigma(s))_n = s_{n+1}$  for  $n \geq 0$ . To show that  $h_{\text{top}}(f) \geq \log 2$ , it is sufficient to show the existence of a semi-conjugacy, namely a continuous surjective map  $h : S^+ \rightarrow \Sigma_2^+$  that makes the diagram below commute.

$$\begin{array}{ccc} S^+ & \xrightarrow{f} & S^+ \\ h \downarrow & \sigma & \downarrow h \\ \Sigma_2^+ & \rightarrow & \Sigma_2^+ \end{array}$$

This function  $h$  gives a combinatorial data of how the orbit of  $x$  visits  $\mathcal{N}$  in time. Once we have shown these properties of  $h$ , it then follows that  $h_{\text{top}}(f) \geq h_{\text{top}}(\sigma) = \log 2$ .

Define  $h : S^+ \rightarrow \Sigma_2^+$  by  $h(x) = (s_0, s_1, s_2, \dots) = s$ , where  $s_n = i$  if  $f^n(x) \in \mathcal{N}_i$  for  $i = 1, 2$ . From the definition,  $h$  is well-defined and makes the diagram commute. For  $h$  to be surjective, we show that

$$\bigcap_{i=0}^{\infty} f^{-i}\mathcal{N}_{s_i} \neq \emptyset \quad (3)$$

for an arbitrary  $s = (s_0, s_1, s_2, \dots, s_n, \dots) \in \Sigma_2^+$ .

*Claim.* There exists a curve  $\alpha_{s_0 s_1} \subset \alpha_{s_0}$  such that  $\rho(f(\text{Im}(\alpha_{s_0 s_1}))) = J_{s_1}$  and  $\rho(f(\partial(\alpha_{s_0 s_1}))) = \partial(J_{s_1})$ .

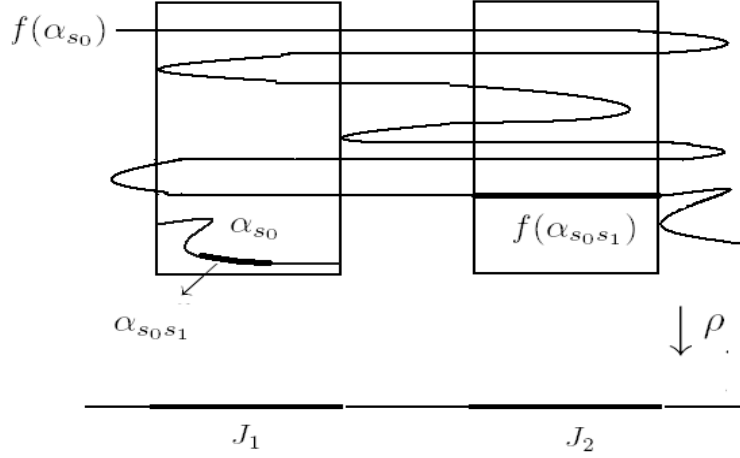


Figure 3: Two curves  $\alpha_{s_0 s_1}$ ,  $\alpha_{s_0}$  and their images under  $f$ . The curve  $\alpha_{s_0}$  satisfies the Lemma and  $\alpha_{s_0 s_1} \subset \alpha_{s_0}$ .

A curve  $\alpha_{s_0}$  that satisfies the Lemma and  $\alpha_{s_0 s_1}$  that illustrates the Claim is given in Figure 3. Inductively, we can construct a nested sequence of compact sets

$$\alpha_{s_0} \supset \alpha_{s_0 s_1} \supset \dots \supset \alpha_{s_0 s_1 \dots s_k} \supset \dots$$

Notice that

$$\bigcap_{n \geq 0} \alpha_{s_0 s_1 \dots s_n} \subset \bigcap_{i=0}^{\infty} f^{-i}(\mathcal{N}_{s_i})$$

and that the left hand side is non-empty. Hence,  $\bigcap_{i=0}^{\infty} f^{-i}(\mathcal{N}_{s_i}) \neq \emptyset$  and thus  $h$  is surjective.

To show that  $h$  is continuous, recall that the topology on  $\Sigma_2^+$  is defined

by the metric

$$d(s, \bar{s}) = \sum_{i=0}^{\infty} \frac{\delta_i}{2^i},$$

where

$$\delta_i = \begin{cases} 0 & \text{if } s_i = \bar{s}_i \\ 1 & \text{if } s_i \neq \bar{s}_i. \end{cases}$$

Since  $\mathcal{N}$  is compact, then for any  $m \in \mathbb{N}$ ,  $f^i$  is uniformly continuous for all  $1 \leq i \leq m$ . Hence, for any  $x, y \in S^+$  that are close,  $f^i(x)$  and  $f^i(y)$  are close in sufficiently long time. Therefore, the symbolic coding for  $h(x)$  and  $h(y)$  agree for a sufficiently long time as well.

**Proof of Theorem 2.** Given a transition matrix  $A$  for  $\mathcal{F}$ , let  $S_A^+ = h^{-1}(\Sigma_A^+) \subset S^+$ , where  $h$  is the map given in the proof of Theorem 1. By definition,  $S_A^+$  is  $f$ -invariant. Showing that  $h : S_A^+ \rightarrow \Sigma_A^+$  is a semi-conjugacy from  $f|_{S_A^+}$  to  $\sigma|_{\Sigma_A^+}$  is essentially the same as the proof of Theorem 1.

## 4 Application to Time Series

### 4.1 Time-Delay Reconstruction

Measuring complex systems frequently do not yield the whole set of state variables but we can infer the missing dynamics from a scalar time series by using the familiar notion of *time-delay technique*, first implemented by Packard, et al. [11]. Let  $\mathcal{M} \subset \mathbb{R}^d$  be bounded,  $f : \mathcal{M} \rightarrow \mathcal{M}$  and  $\rho : \mathcal{M} \rightarrow \mathbb{R}$ , where both  $f$  and  $\rho$  are continuous. For  $m \in \mathbb{N}$ , denote by  $\Gamma_\rho^m$  the reconstruction map of the form

$$\begin{aligned} \Gamma_\rho^m : \quad & \mathcal{M} \rightarrow \mathbb{R}^m \\ x \mapsto \quad & (\rho(x), \rho(f(x)), \dots, \rho(f^{m-1}(x))). \end{aligned}$$

Essentially, only one measurable quantity is needed from the  $d$ -dimensional phase space. From the only quantity that is available, i.e., a sequence of real numbers  $\{u_n\} = \{\rho(x_n)\}$ , the procedure is to construct  $m$ -dimensional vectors and obtain a reconstructed set

$$\mathcal{A}_m = \overline{\{(u_i, u_{i+1}, u_{i+2}, \dots, u_{i+(m-1)}) \mid i \in \mathbb{N}\}}.$$



For  $k \geq 0$ , denote by  $\mathcal{A}_m^k$  the  $k$ th lag of  $\mathcal{A}_m$ , where

$$\mathcal{A}_m^k = \overline{\{(u_i, u_{i+k}, u_{i+2k}, \dots, u_{i+(m-1)k}) \mid i \in \mathbb{N}\}}.$$

If  $\mathcal{M}$  is a compact manifold with  $\dim(\mathcal{M}) = D$ , then for smooth  $f : \mathcal{M} \rightarrow \mathcal{M}$  and  $\rho : \mathcal{M} \rightarrow \mathbb{R}$ , the classical embedding result due to Takens [15] states that under suitable genericity assumptions on the pair  $(f, \rho)$ , if  $N \geq 2D + 1$ , then the map

$$\begin{aligned} \Gamma_\rho^N : \quad \mathcal{M} &\rightarrow \mathbb{R}^N \\ x &\mapsto (\rho(x), \rho(f(x)), \dots, \rho(f^{N-1}(x))) \end{aligned}$$

is an embedding. We shall refer to  $\Gamma_\rho^N$  as the embedding map and  $N$  as an embedding dimension.

## 4.2 Examples

Given  $\{u_n\}$ , we plot in a two-dimensional phase space points of the form  $z_n = (u_n, u_{n+k})$ , with some  $k \geq 1$ . We shall then view the set  $\mathcal{A}_2^k = \overline{\{(u_n, u_{n+k})\}}$  as the graph of the multivalued map  $\mathcal{F}^k : I \rightrightarrows I$ .

### 4.2.1 The Hénon Map

We first consider the two-dimensional Hénon map given by

$$\begin{aligned} x_{n+1} &= 1 + y_n - ax_n^2 \\ y_{n+1} &= bx_n \end{aligned} \tag{4}$$

with initial value  $(x_0, y_0) = (0, 0)$ . Denote by  $\mathcal{H} : I \rightrightarrows I$  the multivalued map from an observation of the Hénon map.

Although it does not matter in principle what set of variables is used in choosing  $\rho$  to do the reconstruction, we obtain a good representation of the true attractor for the Hénon map for  $\rho(x_n, y_n) = x_n$ , as depicted in Figure 4(a). This is because the Hénon map in equation (4) can be written as a second order one-dimensional difference equation given by

$$x_{n+1} = bx_{n-1} + 1 - ax_n^2.$$

Thus, in such a case, the reconstructed set exhibits the exact dynamics of the real system, provided that a good observation function is chosen.

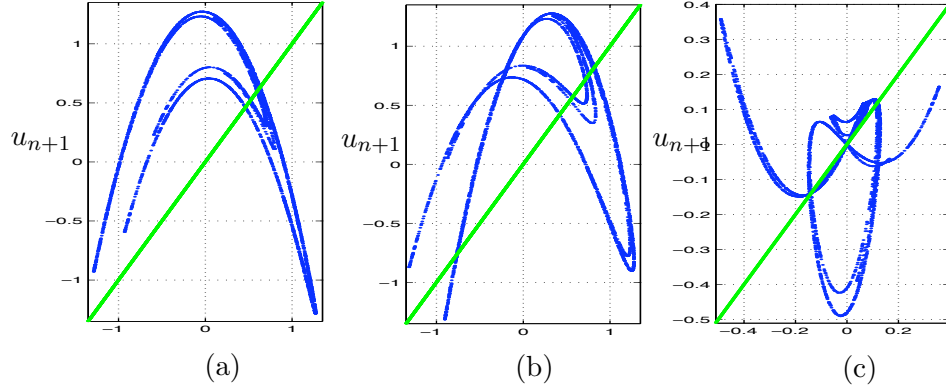


Figure 4: Reconstructed set  $\mathcal{H}_2$  from the Hénon map with  $a = 1.4$ ,  $b = 0.3$ , and for the observation (a)  $\rho(x, y) = x$  (b)  $\rho(x, y) = x + y$  and (c)  $\rho(x, y) = xy$ .

Figure 4 illustrates the graphs of  $\mathcal{H}_2$  for parameters  $a = 1.4$ ,  $b = 0.3$ , and for three different observation functions. Although we do not find intervals that satisfy assumption (\*) given in Theorem 1 for this choice of parameter values, the existence of the intervals is clear for  $\mathcal{H}_2^2$  for parameters  $a = 1.998$ ,  $b = 0.001$ , and observation  $\rho(x_n, y_n) = x_n$ , as depicted in Figure 5(a).

#### 4.2.2 The Magnetoelastic Ribbon

The following example is an application to a time series data coming from a true experiment. The magnetoelastic ribbon is a thin strip of magnetic material whose shape can be changed by applying a magnetic field to it, and this strong coupling between strain and magnetization leads to interesting dynamics. Depending upon the parameters (i.e., the strength of the applied uniform field  $H_{dc}$ , the strength and frequency  $f$  of the applied oscillating field  $H_{ac}$  in the vertical direction), the motion of the ribbon may exhibit a wide variety of different behaviours. For further information concerning the experimental setup, see [12].

We consider two distinct ribbon data which we refer to as ribbon1 and ribbon2. The parameters for ribbon1 are  $H_{dc} = 2212.4542$  mV,  $H_{ac} = 3200$  mV and a driving frequency  $f = .95$  Hz. The parameters for ribbon2 are  $H_{dc} = 2825.3968$  mV,  $H_{ac} = 2840$  mV and  $f = .95$  Hz. Both consist of

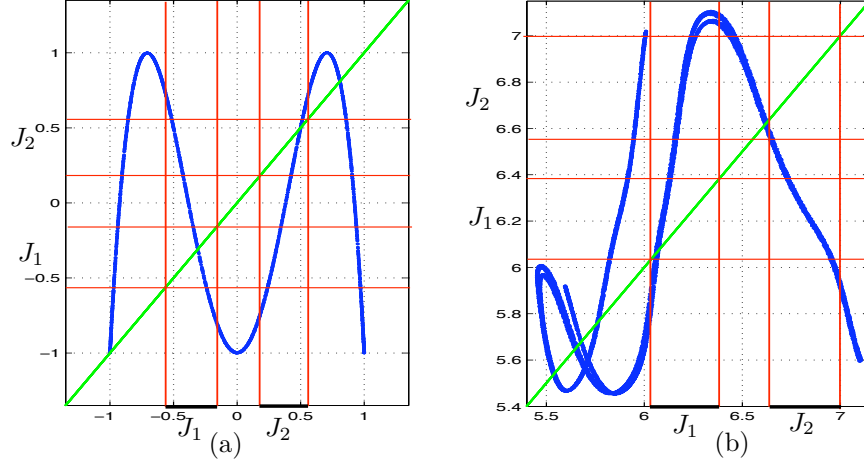


Figure 5: (a) Full shift for the second iterate of the reconstructed Hénon map with  $a = 1.998$  and  $b = 0.001$ . (b) Subshift for the second iterate of the reconstructed magnetoelastic ribbon2 data.

10,000 data points.

For the third iterate  $\mathcal{F}^3$  of the ribbon1 data (refer to Figure 6), we can find  $J_1$  and  $J_2$  that satisfy assumption (\*) in Theorem 1. Although not seen in Figure 6(b), we assume the existence of a continuous selector for  $\mathcal{F}$  over the intervals  $J_1$  and  $J_2$  since ideally, the reconstructed attractor is the closure of infinitely many reconstructed points in  $\mathbb{R}^2$ . Moreover, with the implicit assumption that further increasing the number of data points  $n$  will not alter the intervals that satisfy (\*) for  $\mathcal{F}^3$ , we thus have  $h_{\text{top}}(f) \geq \frac{1}{3} \log 2$ .

Although there are no intervals for which a horseshoe exists for the full shift of the ribbon2 data, we did find a subshift of finite type for the second iterate, associated with the matrix

$$\begin{bmatrix} 1 & 1 \\ 1 & 0 \end{bmatrix}$$

as depicted in Figure 5(b). In this case,  $h_{\text{top}}(f) \geq \frac{1}{2} \left( \frac{1+\sqrt{5}}{2} \right)$ .

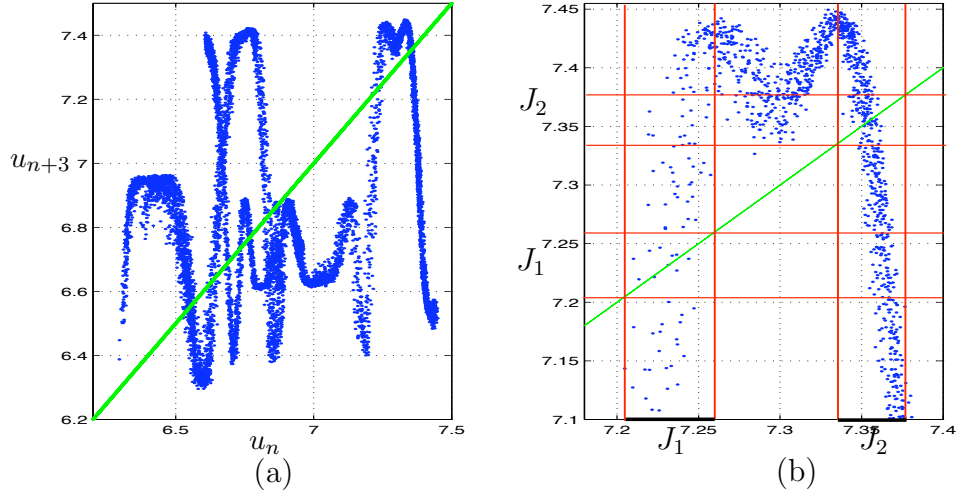


Figure 6: (a) Reconstruction plot for the magnetoelastic ribbon1 data with lag  $k = 3$ . (b) Intervals that satisfy (\*).

## 5 Conclusions

We have presented a method for showing the positivity of the topological entropy of the unknown dynamical system from a one-dimensional reconstruction of time series. By constructing a one-dimensional multivalued map  $\mathcal{F}$  obtained from a time series  $\{u_n\}$ , we can give a lower estimate for the topological entropy of the true dynamical system  $f$ , provided there is horseshoe-like dynamics in  $\mathcal{F}$ .

The advantage of the method presented lies in the fact that we have simplified studying the dynamics in the one-dimensional case and hence *do not need* the reconstruction map to be an embedding. We detect symbolic dynamics through the disjoint intervals satisfying the assumptions in either of the theorems and show that the true system  $f$  is at least as complicated as that of the one-sided full shift or subshift of finite type. Moreover, our method is insensitive to any small error or any small perturbation of  $f$ , say  $f_\lambda$ . This is due to the assumption that  $\mathcal{F}(\partial(J_i))$  will always lie strictly outside  $K$ . This may be argued as well by the robustness of the horseshoe which assures that the graph of  $\mathcal{F}_\lambda$  will lie close to the graph of  $\mathcal{F}$  near the disjoint

intervals satisfying  $(*)$ .

Clearly, the drawback in our method is that the application is restricted to time series data that come from an almost one-dimensional chaotic system. Another weakness of the method is that it is too geometric in detecting the intervals that satisfy the assumptions. Furthermore, we lose information about the geometric information of the true attractor, say  $\mathcal{A} \subset \mathcal{M}$ . In particular, the topology of  $\mathcal{A}$  may not be mirrored in a one-dimensional reconstruction.

## 6 Future Study

Topological entropy has already been established for more general single-valued maps. However, as seen in the examples, many chaotic systems encountered in practice cannot be described by such maps. For a compact metric space  $(X, d)$  and a continuous self map  $f : X \rightarrow X$ , it is known that if  $f$  is a homeomorphism, then  $h_{\text{top}}(f) = h_{\text{top}}(f^{-1})$ . In the case where  $f$  is not invertible, it is worth noting relevant works of Biś, Urbański, Hurley and Nitecki that discuss several entropy-like invariants for noninvertible maps ([2], [3], [6], [10]). They work on backward iterates of a non-invertible map and view the inverse  $f^{-1}$  as a relation. In a similar manner, we can extend this procedure into the *future* and formulate a definition of topological entropy for multivalued maps.

**Definition 6.1** Let  $(X, d)$  be a compact metric space and let  $\mathcal{F} : X \rightrightarrows X$  be a multivalued map. Denote by

$$F_k = \{u = \{u_i, u_{i+1}, \dots, u_{i+k}\}\} \subset X^{k+1} \quad (5)$$

the set of partial orbits of  $\mathcal{F}$  of length  $k$ , i.e.,  $u_{i+l} \in \mathcal{F}(u_{i+l-1})$  for all  $1 \leq l \leq k$ . A set  $F \subset F_k$  is called a  $(k, \delta)$ -separated set for  $\mathcal{F}$  if for any  $u, u' \in F$ ,  $d(u, u') \geq \delta$ .

Let  $S_{\mathcal{F}}(k, \delta)$  be the maximal  $(k, \delta)$ -separated set for  $\mathcal{F}$  with cardinality  $s_{\mathcal{F}}(k, \delta)$ . We define the topological entropy of the multivalued map  $\mathcal{F}$  by

$$h(\mathcal{F}) = \lim_{\delta \rightarrow 0} \limsup_{k \rightarrow \infty} \frac{1}{k} \log s_{\mathcal{F}}(k, \delta). \quad (6)$$

**Proposition 6.1** *Let  $(X, d)$  be a compact metric space and let  $\mathcal{F} : X \rightrightarrows X$  be a multivalued map. Let*

$$Sel^0(\mathcal{F}) = \{g : X' \rightarrow X' | X' \subset X \text{ and } g \text{ continuous}\}.$$

*For any  $g \in Sel^0(\mathcal{F})$ , the following inequality holds*

$$h(\mathcal{F}) \geq \sup\{h(g) | g \in Sel^0(\mathcal{F})\}.$$

As an illustration, we refer again to the reconstructed Hénon map  $\mathcal{H}_2$  with observation function  $\rho(x, y) = x$  given in Figure 4(a). We can choose a branch from  $\mathcal{H}_2$  and consider this as a continuous selector. However, it is worth noting that it is easy to give examples where the lower bound is infinite (e.g., choosing a selector that is too wiggly or erratic) and so we do not get much useful information about the underlying system. To remedy this weakness, we may exclude those selectors that are responsible for high entropy of the system and choose a restricted class of selectors, namely those that are smooth.

## Acknowledgements

The author wishes to acknowledge the support from the Santa Fe Institute during the Complex Systems Summer School 2006. She would also like to thank Prof. Hiroshi Kokubu for the discussions which have been most helpful for the completion of this paper.

## References

- [1] A. Baker, Lower bounds on entropy via the Conley index with applications to time series, *Topology Appl.* **120** (2000) 333-354.
- [2] A. Biś, Entropies of a semigroup of maps, *Discrete and Continuous Dynamical Systems* **11** (2004) 639-648.
- [3] A. Biś and M. Urbański, Some remarks on topological entropy of a semigroup of continuous maps, Preprint, 2003.
- [4] R. Bowen, Entropy for group endomorphisms and homogeneous spaces, *Trans. AMS* **153** (1971) 509-510.

- [5] H.W. Broer, F. Dumortier, S.J. van Strien and F. Takens, *Structures in Dynamics: Finite Dimensional Deterministic Studies*, North-Holland, 1991.
- [6] M. Hurley, On topological entropy of maps, *Ergodic Th. & Dynam. Sys.* **15** (1995) 557-568.
- [7] T. Kaczynski, K. Mischaikow, M. Mrozek, *Computational Homology*, Springer-Verlag New York, 2004.
- [8] K. Mischaikow, M. Mrozek, A. Szymczak and J. Reiss, From time series to symbolic dynamics: an algebraic topological approach, Preprint, 1997.
- [9] K. Mischaikow, M. Mrozek, A. Szymczak and J. Reiss, Construction of symbolic dynamics from experimental time series, *Phys. Rev. Lett.* **82** (1999) 1114-1147.
- [10] Z. Nitecki, Preimage entropy for mappings, *Int. J. Bifur. Chaos* **9** (1999) 1815-1843.
- [11] N. Packard, J. Crutchfield, J. Farmer and R. Shaw, Geometry from a time series, *Phys. Rev. Lett.* **45** (1980) 712-716.
- [12] J. Reiss, The analysis of chaotic time series, Ph.D. Thesis, Georgia Inst. Tech., Atlanta, 2001.
- [13] C. Robinson, *Dynamical Systems: Stability, Symbolic Dynamics, and Chaos*, C.R.C. Press, 1994.
- [14] D. Ruelle, *Chaotic Evolution and Strange Attractors*, Cambridge University Press, 1989.
- [15] F. Takens, Detecting strange attractors in turbulence, *Dynamical Systems and Turbulence, Warwick 1980*, D. Rand and L. S. Young, eds., Lecture Notes Math. **898**, Springer-Verlag, Berlin, 1981.